MOLECULAR AND CELLULAR BIOLOGY, Feb. 1997, p. 529–536 Vol. 17, No. 2
0270-7306/97/$04.00+0

Transcription-Dependent Induction of G_1 Phase during the Zebra Fish Midblastula Transition

ELI ZAMIR, ZVI KAM, AND ANAT YARDEN*

Department of Molecular Cell Biology, The Weizmann Institute of Science, Rehovot 76100, Israel

Received 23 July 1996/Returned for modification 21 August 1996/Accepted 30 October 1996

The early development of the zebra fish (*Danio rerio*) embryo is characterized by a series of rapid and synchronous cell cycles with no detectable transcription. This period is followed by the midblastula transition (MBT), during which the cell cycle gradually lengthens, cell synchrony is lost, and zygotic transcription is initially detected. In this work, we examined the changes in the pattern of the cell cycle during MBT in zebra fish and whether these changes are dependent on the initiation of zygotic transcription. To characterize the pattern of the early zebra fish cell cycles, the embryonic DNA content was determined by flow cytometric analysis. We found that G_1 phase is below detection levels during the first 10 cleavages and can be initially detected at the onset of MBT. Inhibition of zygotic transcription, by microinjection of actinomycin D, abolished the appearance of G_1 phase at MBT. Premature activation of zygotic transcription, by microinjection of nonspecific DNA, induced G_1 phase before the onset of MBT, while coinjection of actinomycin D and nonspecific DNA abolished this early appearance of G_1 phase. We therefore suggest that during the early development of the zebra fish embryo, G_1 phase appears at the onset of MBT and that the activation of transcription at MBT is essential and sufficient for the G_1-phase induction.

Following fertilization, the early embryonic cell cycles of certain organisms (i.e., *Drosophila melanogaster* and *Xenopus laevis*) are very short and synchronous. During these cycles, alterations between DNA replication (S phase) and mitosis (M phase) are observed, with no detectable G_1 or G_2 phase of the cell cycle (7, 9). This period is also uniquely characterized by the absence of transcription (6, 22). Subsequently, at the midblastula transition (MBT), the cell cycle gradually lengthens, cell synchrony is lost, and zygotic transcription is initially detected (4, 9, 21, 22). The zebra fish (*Danio rerio*) embryo follows this pattern: immediately after fertilization, the zygote undergoes seven rapid and synchronous cellular divisions, followed by slight metasynchrony, with waves of mitosis emanating from the animal pole (15, 16). During this stage, there is a gradual increase in the cell cycle length (19). At the 10th cleavage, the beginning of the MBT, three spatially separate mitotic domains with distinctive cell cycle lengths appear (14). The pattern of the cell cycle which is acquired during this transitional stage, the involvement of zygotic transcription, and the molecular mechanisms which govern the exit from the fast M/S cleavage cycles are not known.

The initiation of MBT has been suggested to be triggered at a critical nucleocytoplasmic ratio (4, 13, 21). During early development, this ratio increases exponentially as a function of the cycle number, since the total volume of the cytoplasm remains constant while genomic DNA replicates during each cell cycle. The question of whether the two major events which initiate at MBT, transcription activation and cell cycle lengthening, occur independently, or one event is the cause of the other, is one of the fundamental open questions in early development. Both events probably sense the nucleocytoplasmic ratio, by titration of maternal components which interact with the exponentially increasing amounts of DNA. Two different mechanisms have been suggested to take place in *Drosophila* and *Xenopus* embryos. It has been shown that in the *Drosophila* embryo, cell cycle lengthening precedes zygotic transcription activation, and it has been suggested that as the cell cycle elongates, more time is given for transcription complexes and reactions to be established (4, 6). In *Xenopus*, lengthening of the cell cycle at MBT appears to be independent of transcription activation. Transcriptional inhibition, caused by injection of α-amanitin into *Xenopus* embryos, had no effect on cell cycle lengthening at MBT (21), and inhibiting the embryonic cell cycles did not cause transcriptional activation (24). Suppression of the interaction between the transcriptional machinery and the DNA before MBT has been attributed to an excess of maternal histones (17, 22, 24). Indeed, an artificial increase in the DNA content prior to MBT, by microinjection of nonspecific DNA, induced earlier transcription of class III genes and some class II genes (1, 22–24). However, it is still not known if this premature transcription activation is accompanied by premature cell cycle lengthening. Furthermore, the mechanisms responsible for cell cycle elongations in *Xenopus*, or any other vertebrate, remain to be determined.

The cell cycle pattern (namely, the relative length of each phase of the cell cycle) which is acquired as the cell cycle elongates at MBT has been extensively studied in *Drosophila*. It was shown that G_1 phase is absent at the *Drosophila* MBT (20). In addition, G_2 phase was shown to initially appear in the *Drosophila* cycle 14 (5), while G_1 phase was shown to initially appear following mitosis 16 in neural and imaginal discs (10). Much less is known about the cell cycle pattern which is acquired as the cell cycle elongates in other species. In *Xenopus*, both G_1 and G_2 phases were initially detected at the late blastula stage, about 1 h after MBT (9), while G_1 phase was reported to appear much later, at the gastrula stage (at 10 h postfertilization) (8).

To study the transitions in the cell cycle pattern which take place during zebra fish embryogenesis, we have analyzed the cell cycle distribution by flow cytometry. From quantitation of the DNA content of embryonic nuclei at various developmen-

* Corresponding author. Mailing address: Department of Molecular Cell Biology, The Weizmann Institute of Science, Rehovot 76100, Israel. Phone: 972-8-9342289. Fax: 972-8-9469713. E-mail: lianat@weizmann.weizmann.ac.il.

tal stages, we were able to demonstrate that G_1 phase is initially detected at MBT. Furthermore, we show here for the first time that this induction of G_1 phase in the zebra fish embryo depends on activation of zygotic transcription.

MATERIALS AND METHODS

Maintenance of fish and embryos. Zebra fish were raised at the Weizmann Institute fish facility (2) essentially as described by Westerfield (32). Adult fish were maintained in charcoal-filtered, double-distilled water supplemented with salts (3). Embryos were obtained by mating four males and two females over marbles as described previously (32). Following cleaning and staging, embryos were incubated in fish water at 28.5°C as described by Westerfield (32). Embryos at either two-, four-, or eight-cell stage were kept separately at 28.5°C, thus creating populations of embryos spanning evenly within one cell cycle.

Microinjection. Embryos, in their chorions, at the 2- to 16-cell stage were microinjected in an agarose mold under a dissection microscope (32). Glass capillaries (1 mm fiber filled; WPI, Sarasota, Fla.) were pulled in a horizontal puller (Sutter Instruments, San Rafael, Calif.) and mounted on a Leitz (Wetzlar, Germany) micromanipulator connected to a semiautomatic microinjector (Eppendorf 5242; Eppendorf, Hamburg, Germany). The injected solution (0.2 or 0.02 μg of actinomycin D [Sigma] per ml, 1 μg of Bluescript plasmid DNA per ml, or 10 μCi of [α-^{32}P]UTP [DuPont NEN, Bad Homburg, Germany] per ml in 0.05% phenol red) was introduced between the cells and the yolk. The injection volume was approximately 5 nl. Injected embryos were maintained at 28.5°C for a set time (designated hours postfertilization [hpf] in accordance with the staging of Westerfield [32]). For time-lapse recording, either water or actinomycin D was microinjected as described above. Embryos were kept in the agar mold at 28.5°C and recorded with a video camera (JVC, Tokyo, Japan) digitized by a Scion (Frederick, Md.) card, using NIH Image. For Nomarski optics, actinomycin D-injected embryos at the desired stage were transferred from the agar mold into a depression slide, and pictures were taken by using water-immersion objectives (10× numerical aperture of 0.3 or 40× numerical aperture of 0.75) attached to an Axiophot light microscope (Zeiss, Oberkochen, Germany).

Flow cytometric DNA content analysis. Zebra fish embryos were transferred from 28.5°C to ice-cold calcium-free Ringer solution (116 mM NaCl, 2.9 mM KCl, 5 mM HEPES [pH 7.2]) in a transparent cooled chamber under a dissection microscope. The chamber was kept at 1°C by a circulation of ice-cold water. This arrested development simultaneously for all the embryos and allowed time for dechorionation and separation of blastomere cell caps from the yolk. Changes in DNA content distributions were observed when this process was done at room temperature (data not shown). Embryonic cell caps were transferred to a siliconized Eppendorf tube containing 500 μl of ice-cold calcium-free Ringer solution. Suspension of the cells was performed by gentle pipetting, followed by 15 min of incubation in 0.1% Triton X-100 and 400 μg of RNase A and staining with 1 mg of propidium iodide (Sigma) per ml. Following filtration through 50-μm nylon mesh, the stained nuclear suspension was analyzed by a FACSort flow cytometer (Becton Dickinson, San Jose, Calif.) or a FACScan or FACStarplus flow cytometer (Becton Dickinson). During flow cytometric analysis, nuclear suspensions were kept constantly on ice. In each experiment, an average of 1,000 nuclei (from 12 to 20 embryos) were analyzed per point, except for the single-embryo analysis. A suspension of nuclei prepared from adult zebra fish liver as described above was used for calibration of the 2N DNA content population (Fig. 1). DNase treatment (50 U of DNase I [Boehringer, Mannheim, Germany] in 0.1 M $MgCl_2$, 8-hpf embryos) was used as a control (Fig. 1). DNA histograms were deconvoluted according to a simple three-component model which we wrote assuming that S-phase nuclei distribute equally between 2N and 4N DNA content and that nuclei in G_1 phase or in G_2 + M phases contribute superimposed distributions around the 2N or 4N DNA content, respectively. DNA content histograms of single embryos at 8 hpf were deconvoluted by the RFIT model (cellFIT software; Becton Dickinson).

RNA measurements. RNA was extracted from embryos which were microinjected with ^{32}P-labeled UTP (800 Ci/mmol; NEN), in the presence or absence of actinomycin D (0.2 μg/μl), at 3.5 hpf as described by Kane and Kimmel (13). However, radiolabel incorporation was detected on air-dried filters without scintillation fluids.

Protein analysis. Proteins were extracted from zebra fish embryos in radioimmunoprecipitation assay buffer (50 mM Tris-HCl [pH 7.5], 150 mM NaCl, 5 mM EDTA, 1% sodium deoxycholate, 1% Triton X-100) containing 1 mM phenylmethylsulfonyl fluoride, 10 μg of leupeptin per ml, 10 μg of pepsin per ml, 20 μg of aprotonin per ml, 10 μM $NaPP_i$, 50 μM NaF, and 0.5 mM $NaVO_4$. Single actinomycin D (0.2 μg/μl)-injected embryos at the desired stage were placed in 40 μl of radioimmunoprecipitation assay buffer at 4°C, sonicated, and loaded onto a 10% polyacrylamide gel (one embryo equivalent [approximately 40 μg] per lane). Blotting was carried out for 1 h in 50 mM Tris–50 mM glycine–1 mM $MgCl_2$ at 200 mA onto Hybond-C (Amersham, Little Chalfont, England) at 0 to 4°C. The filter was incubated with an anti-proliferating cell nuclear antigen (PCNA) monoclonal antibody (clone PC-10, at a 1:3 × 10^3 dilution; Sigma ImmunoChemicals, St. Louis, Mo.). Detection of bands was carried out by using peroxidase-coupled goat anti-rabbit antibodies and the Amersham ECL (enhanced chemiluminescence) system.

RESULTS

Cell cycle analysis of zebra fish embryos at different developmental stages. To characterize changes in cell cycle patterns during various developmental stages of the zebra fish embryo, we have used flow cytometric DNA content analysis. Zebra fish embryos were precisely staged as described in Materials and Methods and kept at 28.5°C until reaching the desired stage, timed as described by Westerfield (32). At this time, suspensions of nuclei were prepared and stained with propidium iodide for flow cytometric analysis. The nuclear population was separated from fragments and aggregates by gating out the small particles, using dot plots of fluorescence width versus fluorescence area (Fig. 1, column A, R1 population), and by microscopic observation of the sorted population, which revealed that it consisted of isolated nuclei and free of clumps and debris (data not shown). The positive correlation between the nuclear DNA content (represented by the fluorescence height) and the particle size (represented by the forward scatter) of the R1-gated population enabled additional gating (Fig. 1, column B, R2 population). A subpopulation with relatively low forward scatter was identified at early developmental stages (Fig. 1, column B, R3 population). This subpopulation may represent an advanced stage of mitosis, during which the chromatin becomes more condensed and appears smaller and whose relative time length is significantly greater during the early embryonic cycles (see also Fig. 5).

Histograms of fluorescence height of R1- and R2-gated populations represent the DNA content distribution of the embryonic nuclear suspension (Fig. 1, column C). The fluorescence height of the 2N DNA content was verified by using suspensions of nuclei prepared from zebra fish liver cells (G_1 arrested) (Fig. 1, samples 8). In addition, the specificity of the propidium iodide fluorescence height as an indication of intact DNA content in the nuclear suspensions was demonstrated by DNase I treatment, which abolished the 2N and 4N fluorescence intensity peaks, creating a typical distribution of fragments (Fig. 1, sample 7, DNase).

During the cleavage stage (0 to 3 hpf), the fluorescence height histograms lack a peak at the 2N DNA content position. Deconvolution of the DNA content histograms showed that during these early stages, approximately 35% of the population is uniformly distributed between 2N and 4N, while approximately 63% has a DNA content of 4N (Fig. 1, column C, samples 1 and 2; Table 1). Thus, the relative length of G1 before MBT is negligible (Table 1). At the onset of MBT (2K cell stage, 3.25 hpf), a cell population with 2N DNA content starts to accumulate, indicating the initial appearance of a G_1 phase in the zebra fish embryo (Fig. 1, samples 3). Deconvolution of the fluorescence height histograms indicates that the 2N cell population becomes statistically significant at MBT (Table 1). Together with the appearance of G_1 phase at MBT, the absolute length of S phase dramatically increased while the absolute length of G_2 + M phases decreased (Table 1). The 2N population gradually increased during development, as indicated by the cell cycle analysis of embryos at 3.67, 4, and 8 hpf (Fig. 1, samples 4 to 6).

Cell cycle analysis of actinomycin D-injected zebrafish embryos. Since both zygotic transcription and G_1 phase appear at the onset of MBT (reference 13 and Fig. 1, respectively), we checked the possible causal relationship between them by analyzing the cell cycle distribution when transcription was inhibited. Microinjection of the transcriptional inhibitory drug actinomycin D into young (2- to 16-cell-stage) zebra fish embryos inhibited the incorporation of [α-^{32}P]UTP as expected (Fig. 2B) and abolished the appearance of G_1 phase at the onset of

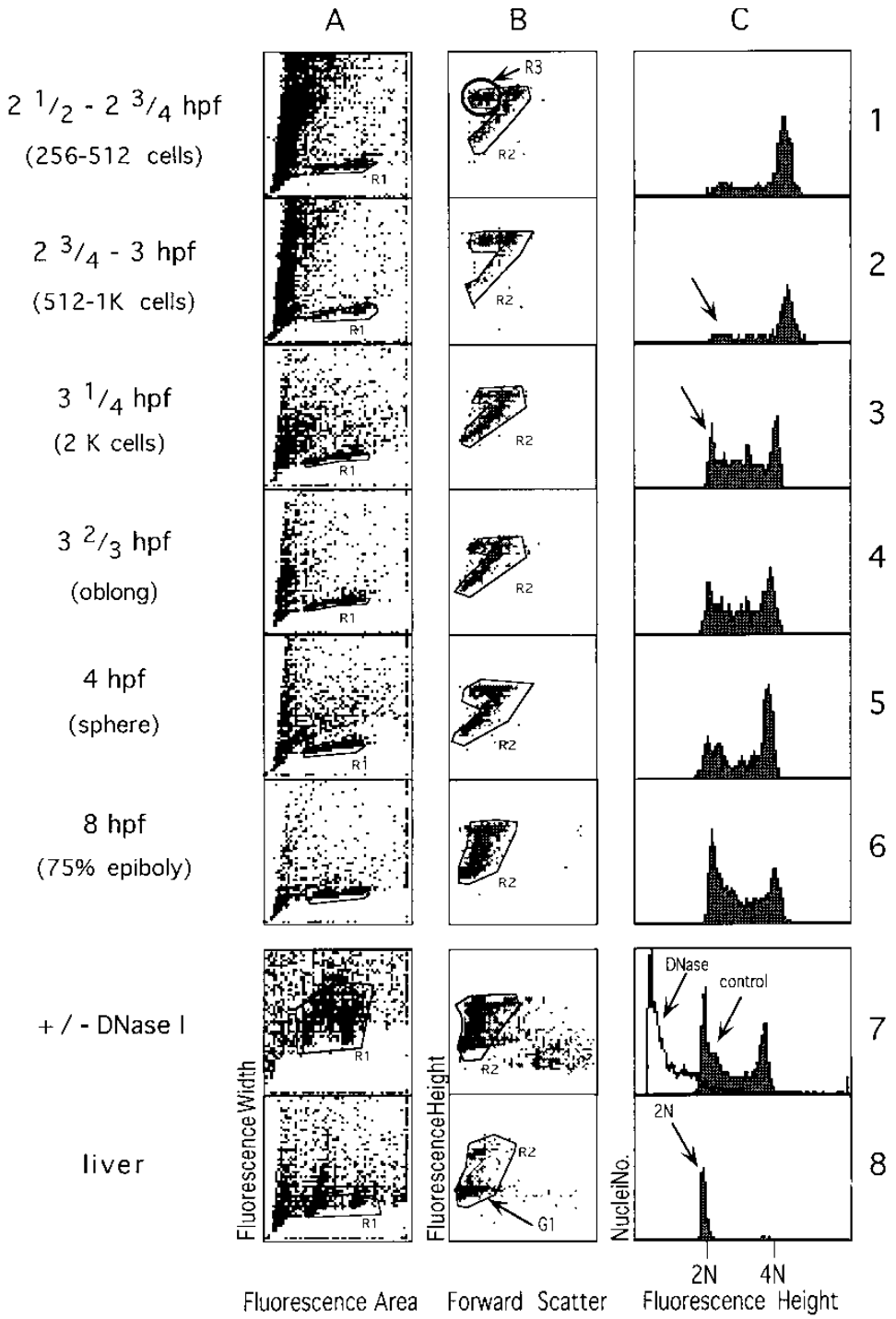

FIG. 1. Cell cycle analysis of embryos at different developmental stages. For each experiment, a suspension of nuclei was prepared from 12 to 20 embryos for flow cytometry DNA content analysis. (A) Dot plots of fluorescent width versus fluorescent area of all the acquired events. Region R1 was defined to exclude clumps of nuclei and debris. (B) Dot plots of fluorescent height versus forward scatter of R1-gated events. The dot plot displays a well-defined population (in the shape of the number 7) around which region R2 was defined. (C) DNA content histograms as reflected by the fluorescent height histograms of R1- and R2-gated events. Rows 1 to 6, embryos at successive developmental stages; row 7, suspensions of nuclei, prepared from embryos at 8 hpf, incubated with DNase buffer (dot plots, columns A and B) with or without DNase I as indicated by the arrows (histogram, column C); row 8, suspension of nuclei prepared from an adult fish liver. Arrows in rows 2 and 3 point to the locations of DNA content of 2N.

MBT (Fig. 2A). Deconvolution of the DNA content histograms indicated that G_1 phase was below detection levels in the actinomycin D-injected embryos, in contrast to the dye-injected control embryos analyzed in parallel (Table 1). In addition, actinomycin D had no effect on the cell cycle distribution during the cleavage stage and specifically abolished the appearance of G_1 phase at the onset of MBT without affecting the elongations in S phase during the same time (Fig. 2A;

TABLE 1. Percentage of nuclei in each phase of the cell cycle at the blastula stage and following the introduction of actinomycin D and/or nonspecific DNA

hpf	Treatment	n^a	% of nuclei (mean ± SD) at [b]:		
			G_1	S	G_2 + M
2.5–2.75	—[c]	7	1.7 ± 2.7	35 ± 18	63 ± 19
3.25–3.5	—	4	6.8 ± 1.7	77.9 ± 6	15.3 ± 5.5
3.25–3.5	AMD[d]	3	0.5 ± 0.7	76.5 ± 5.7	23 ± 6.3
2.25–2.5	NS-DNA[e]	3	25.2 ± 8.7	52 ± 10.6	22.8 ± 2.6
2.25–2.5	NS-DNA + AMD[e]	2	0 ± 0	56.4 ± 11	43.6 ± 11

[a] Number of repeated experiments.
[b] Calculated from the DNA content histograms by our deconvolution model to estimate the percentage of G_1, S, and G_2 + M phases.
[c] —, some of the nontreated experimental data include embryos which were microinjected with 0.05% phenol red in water. Such treatment did not change the cell cycle distribution.
[d] Embryos were microinjected with 0.2 μg of actinomycin D (AMD) per μl.
[e] Embryos were microinjected with 1 μg of nonspecific plasmid DNA (NS-DNA) alone or with 0.2 μg of actinomycin D per μl.

Table 1). Therefore, we conclude that the initial appearance of G_1 at the onset of MBT depends on the induction of zygotic transcription, while the elongation of S phase is not influenced by the transcriptional activity during this time point in zebra fish embryonic development.

It should be mentioned that actinomycin D was not toxic to the embryos at MBT. In actinomycin D-injected embryos, MBT was not retarded (Fig. 3A, B, and D), and developmental abnormalities were observed only at the initiation of gastrulation (Fig. 3C and F). Moreover, the actinomycin D-injected embryos had PCNA levels similar to those of control embryos at 4 hpf (Fig. 3E, inset), giving an additional indication that at this stage, actinomycin D-injected embryos were not different from normal embryos. The levels of PCNA in the actinomycin D-injected embryos declined at 5 hpf (Fig. 3E, inset), at the same time as embryonic abnormalities started to appear in the injected embryos (Fig. 3F). It is interesting that when 10-fold less actinomycin D was injected, developmental abnormalities appeared only at later stages (Fig. 3C).

Cell cycle analysis of DNA-injected zebra fish embryos. Introduction of nonspecific plasmid DNA into *Xenopus* embryos at the blastula stage was previously shown to cause premature activation of zygotic transcription, possibly via titration of some maternal repressors (22, 24). To check whether premature transcriptional activation is sufficient to induce G_1 phase at earlier developmental stages in the zebra fish embryo, we microinjected nonspecific plasmid DNA into young (4- to 16-cell-stage) zebra fish embryos and analyzed their cell cycle distribution at the 256- to 512-cell stage. The amount of the injected nonspecific DNA per embryo was approximately equivalent to the DNA content of a 1K-cell-stage embryo (5 ng/embryo). Cell cycle analysis of the nonspecific DNA-injected embryos indicated that a population with a DNA content of 2N appeared prematurely at the 2.5- to 2.75-cell stage (Fig. 4; Table 1). Moreover, this premature appearance of G_1 phase could be abolished by coinjection of actinomycin D together with the nonspecific DNA (Fig. 4). Therefore, the premature induction of G_1 phase is probably mediated by the premature activation of zygotic transcription.

It should be noted that the absolute length of S phase was not affected by the introduction of the nonspecific DNA (Table 1), demonstrating that also in this case, the induction of G_1 phase was specifically affected by the activation of zygotic transcription.

Cell cycle analysis of single embryos at MBT. To check whether the cells which enter G_1 phase at the onset of MBT form a subpopulation of 2N arrested cells or only transiently pass through G_1 phase, single-embryo analysis was carried out. The DNA content histograms of single embryos, at the 1K- and 2K-cell stages, were found to be different from each other and from the DNA content histogram of a pool of 20 embryos at the same stage (Fig. 4). These histograms reflect the metasynchronic cell cycles within a single embryo at this stage and show single embryo either at S phase (Fig. 5, sample 5) or at various stages during M phase, with a DNA content of either 4N or 4N and 2N (Fig. 5, samples 1 to 4). Among some of the mitotic embryos, a subpopulation, termed previously R3 (Fig. 1), could be identified. This R3 population probably reflects a late stage in mitosis (anaphase). Since the 2N population did not appear in all single embryos analyzed (e.g., samples 1 and 2 in Fig. 5), we suggest that all cells which enter G_1 continue to cycle at MBT.

DISCUSSION

We have used flow cytometric DNA content analysis to characterize changes in cell cycle patterns during zebra fish embryonic development. We found that following the initial 10 M/S cycles of the cleavage stage, G_1 phase appears at the onset

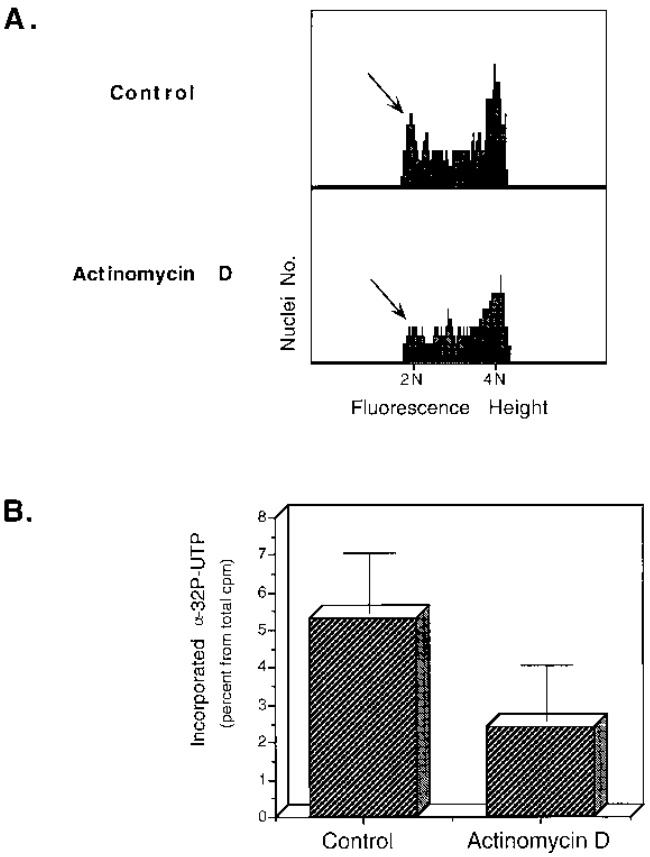

FIG. 2. Effects of actinomycin D on the cell cycle pattern, on UTP incorporation, and on embryonic development at MBT. (A) DNA content histograms of embryos which were microinjected with control or actinomycin D (0.2 μg/μl) and incubated at 28.5°C until 3.25 to 3.5 hpf. Arrows point to the locations of DNA content of 2N. (B) Incorporation of [α-^{32}P]UTP into embryos which were microinjected with [α-^{32}P]UTP alone or together with actinomycin D (0.2 μg/μl). The embryos were incubated at 28.5°C until 3.25 to 3.5 hpf, RNA was extracted, and the ratio between incorporated and total [α-^{32}P]UTP was measured. Standard deviation was calculated from four repeated experiments.

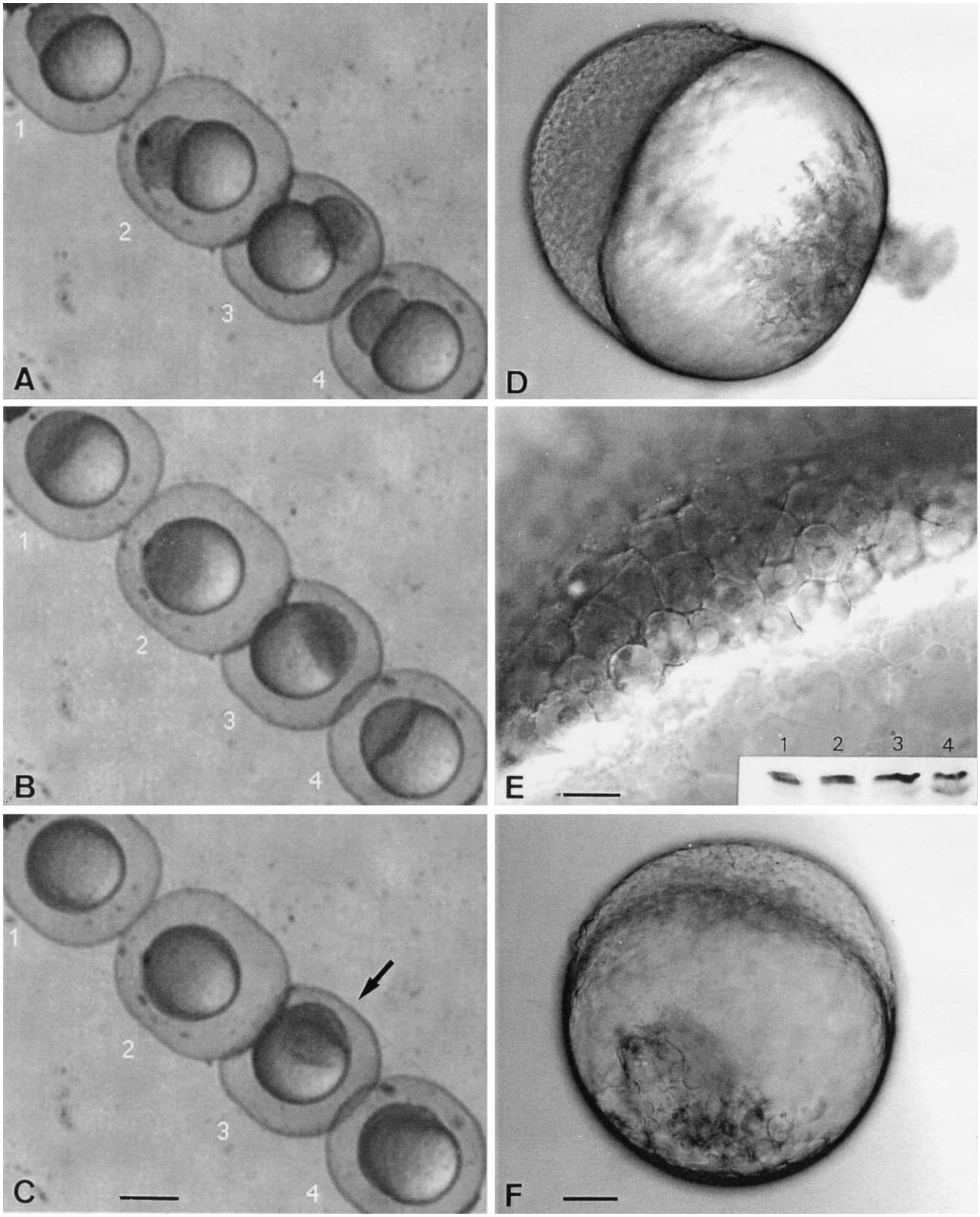

FIG. 3. Effect of actinomycin D on embryonic development. (A to C) Video time-lapse recording of embryos which were microinjected with control dye or with actinomycin D. Embryos (placed in an agar mold) were microinjected with 5 nl of 0.05% phenol red alone (embryos 1 and 2) or with 0.2 (embryo 3) or 0.02 (embryo 4) μg of actinomycin D per ml and videotaped, using NIH Image. Frames of embryos at the 128-cell stage (2.25 hpf; A), at the dome stage (4.33 hpf; B), or at the shield stage (6.67 hpf; C) are shown. Note retarded development of embryo 3 (marked with an arrow in panel C). Bar = 300 μm. (D to F) Actinomycin D-injected embryos as observed with Nomarski optics. Embryos were microinjected with 0.2 μg of actinomycin D per ml and incubated at 28.5°C for 3.75 h (D and E) or 5 h (F). Bars = 10 μm (E) and 100 μm (F). The inset in panel E shows Western blot analysis of single zebra fish embryos (approximately 40 μg/lane) which were injected with actinomycin D (0.2 μg/μl; lanes 2 and 4) or with control dye (lanes 1 and 3) and incubated at 28.5°C for 4 h (lanes 1 and 2) or 5 h (lanes 3 and 4). The blot was reacted with anti-PCNA monoclonal antibody PC-10.

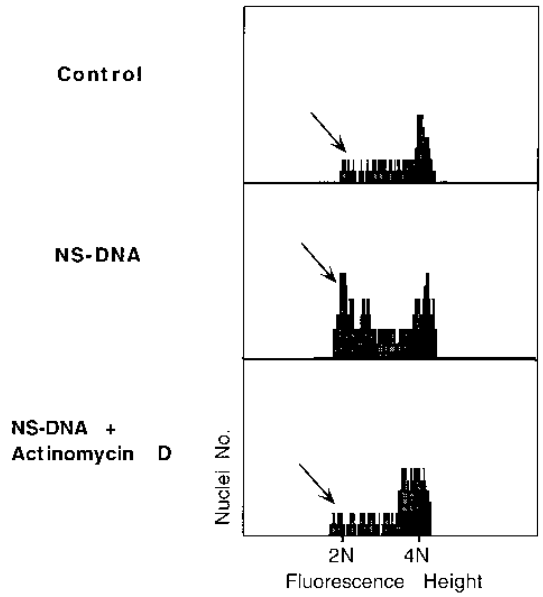

FIG. 4. Effect of nonspecific DNA on the cell cycle pattern before MBT. DNA content histograms of embryos which were microinjected with control, nonspecific DNA (NS-DNA) or nonspecific DNA (NS-DNA) plus actinomycin D (0.2 μg/μl). The embryos were incubated at 28.5°C until 2.5 to 2.75 hpf. Arrows point to the locations of DNA content of 2N.

of MBT. This induction is accompanied with an increase in the percentage of cells in S phase, which together with G_1 phase contributes to the overall elongation of the cell cycle. G_1-phase induction depends on the activation of zygotic transcription, while the elongation in S phase occurs even when transcription is inhibited.

Cell cycle lengthening at the zebra fish MBT was previously shown to occur due to lengthening of interphase (13), but the contribution of each phase to this lengthening has not been determined. Here we demonstrate, for the first time, that G_1 phase of the cell cycle initially appears at the onset of the zebra fish MBT (Fig. 1; Table 1). Our estimation is that on average, 6% of the nuclei are at the G_1 phase during 3.25 to 3.5 hpf. We cannot discriminate between two situations: either all of the cells spend 6% of their cycle in G_1 phase or only a fraction of the cells spend more time at the G_1 phase. It has previously been shown that lengthening of the cell cycle at MBT occurs cell autonomously, resulting in loss of cell synchrony (13, 14). Moreover, the median cell cycle length at MBT was shown to increase by 24.4% (17 min in cycle 10 and 22.5 min in cycle 11 [13]). Therefore, we suggest that at MBT, more than 6% of the embryonic cells enter G_1 phase, while other cells will add G_1 phase to their cycle at the subsequent stages.

The appearance of G_1 phase at MBT occurs concomitantly with the onset of zygotic transcription in the developing zebra fish embryo (13). Here we demonstrate, for the first time, a causal relationship between these two events. We show that by inhibiting zygotic transcription with actinomycin D, the induction of G_1 phase was abolished. Furthermore, following the introduction of nonspecific DNA into zebra fish embryos at the blastula stage, G_1 phase appeared prematurely before MBT (Fig. 1), and this induction of G_1 phase could be abolished by coinjection of actinomycin D together with the nonspecific DNA. Thus, we concluded that transcriptional activation is essential and sufficient for inducing G_1 phase at MBT in zebra fish.

The absolute length of G_1 phase, induced before MBT by nonspecific DNA, is significantly longer then the length of G_1 at MBT (Table 1; Fig. 4). This observation raises the possibility that the induction of G_1 phase at MBT is accompanied by additional developmentally regulated cell cycle events. In the case of artificial induction of G_1 phase as well as zygotic transcription, by microinjection of nonspecific DNA, it is possible that the transition from G_1 phase to S phase is slower than the transition which naturally occurs at MBT. It is possible, for example, that products of genes transcribed at MBT regulate the G_1/S transition or that degradation or posttranscriptional accumulation of factors which regulate the G_1/S transition occurs during MBT, influencing the length of G_1.

A critical ratio between the DNA content and the volume of the cytoplasm was shown to be required for the induction of zygotic transcription (6, 13, 21). Here we showed that the induction of G_1 depends on the induction of zygotic transcription, suggesting that both events may take place in the same embryonic cells at MBT. The nucleocytoplasmic ratio can be influenced by the cell size; thus, in smaller cells, transcription and G_1 phase may occur earlier than in larger cells. Another parameter which can influence the induction of zygotic transcription may be the distance from the yolk sac. The yolk sac contains the maternal supply, probably including putative transcriptional repressors. Cell layers which are located away from the yolk may contain less of the putative repressors, and in such cells, transcription and G_1 phase may appear earlier. For example, the cells of the enveloping layer may be the first population to have G_1 phase, in contrast to the yolk syncytial layer, which shares cytoplasm with the yolk sac. Indeed, it was previously reported that the cell cycle of the enveloping layer is slower than that of the yolk syncytial layer or the deep-cell layer (13, 14). It is interesting that the enveloping-layer cells are the first to adhere to each other. Organized cell-cell contacts were initially detected in the enveloping layer at the 1K cell stage by whole-mount immunostaining of actin, α-actinin, and vinculin (22a). This observation may link formation of cell-cell contacts to growth inhibition as previously suggested for density-dependent inhibition in monolayers of tissue culture cells (30).

In addition to the appearance of G_1 phase at MBT, a dramatic increase in the absolute length of S phase was observed (Table 1). Lengthening of S phase at MBT is probably not a result of transcription activation, since microinjection of nonspecific DNA or actinomycin D had no effect on the absolute length of S phase (Table 1). It is possible that the maternal stock of the DNA replication machinery gradually became a limiting factor for S phase at MBT. This could be due to degradation or dilution of the maternal factors. Furthermore, actinomycin D-injected embryos continued to develop up to gastrulation (Fig. 3), indicating that G_1-phase induction, as well as transcription, is not rate limiting for development at MBT. Similarly, it has also been demonstrated that in both *Xenopus* and *Drosophila*, lengthening of the cell cycle does not depend on novel zygotic transcription (4, 21). The transcriptionally dependent induction of G_1 phase and the transcriptionally independent elongation of S phase together contribute to cell cycle lengthening at the zebra fish MBT.

Based on the results presented here, we suggest that novel zygotic transcripts inhibit the immediate entry into S phase, following the completion of mitosis 10, and thereby induce G_1 phase. This transcript may be one of the cyclin-dependent kinase (CDK) inhibitors which interact stoichiometrically with cyclin-CDK complexes and prevent their enzymatic activity (reviewed in reference 12 and 29). Induced transcription of this CDK inhibitor (CKI) may inhibit entry into S phase by negatively regulating the activity of an S-phase-specific CDK, lead-

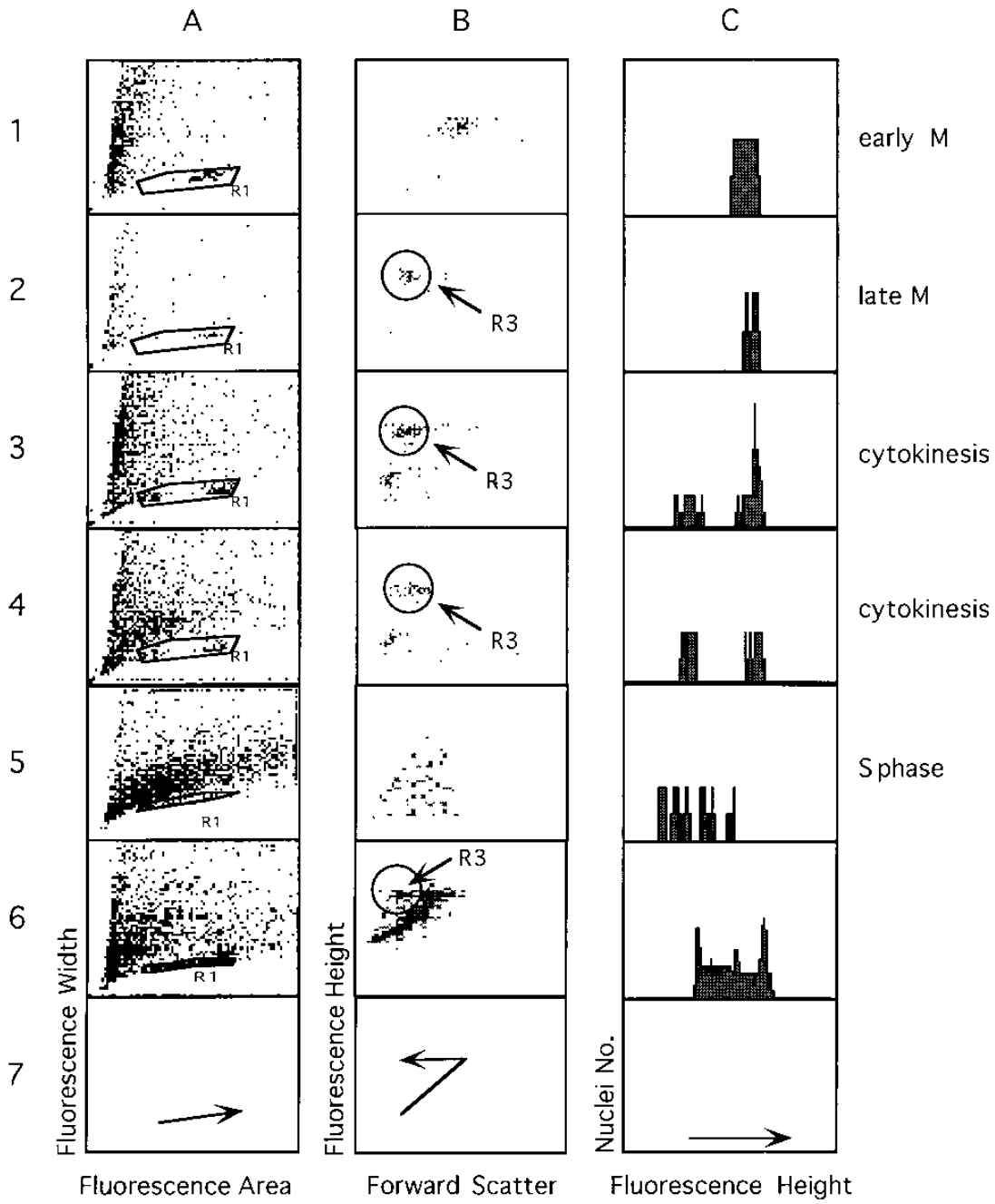

FIG. 5. Cell cycle analysis of single embryos at 3 to 3.25 hpf. (A) Dot plots of fluorescent width versus fluorescent area of the total events. Region R1 was defined to exclude clumps of nuclei and debris. (B) Dot plots of fluorescent height versus forward scatter of R1-gated events. (C) DNA content histograms as reflected by the fluorescent height histograms of R1-gated events. Rows 1 to 5, for each experiment, a suspension of nuclei was prepared from a single embryo and assigned in the order of the corresponding cell cycle phase (as marked on the right); row 6, a suspension of nuclei was prepared from 20 embryos; row 7, arrows indicate the pathway that nuclei pass in the different graphs while progressing in the cell cycle, starting with the beginning of interphase and ending at the beginning of cytokinesis.

ing to the appearance of G_1 phase at MBT. In that context, it is interesting that one of these CKIs, $p21^{CIP1}$, was shown to be transactivated by MyoD (11) and that transcription of MyoD itself was shown to be induced at MBT in *Xenopus* (26). Alternatively, this novel transcript may be the transcript encoding the product of the retinoblastoma susceptibility gene (pRb) or its family members p107 and p130, which negatively regulate the transition from G_1 into S phase (for reviews, see references 27 and 31). Since in this work we show that the embryonic cells which enter G_1 phase continue to cycle and are not cell cycle arrested at MBT (Fig. 5), a molecular mechanism which positively regulates the G_1/S transition should also be present at MBT. We previously reported that the zebra fish cyclin D1 transcripts could be initially detected during this time (33). This G_1 cyclin is known to positively regulate the G_1/S transition (reviewed in reference 28) through negative regulation of pRb function by phosphorylation (18, 25). Thus, transcription of either one of the CKIs or one of the pRb family members

might be responsible for the appearance of the G_1 phase at the zebra fish MBT, while transcription of cyclin D1 at the same time ensures that cells do not arrest in G_1 and continue to cycle.

ACKNOWLEDGMENTS

We thank B. Geiger for continuous support and for many fruitful discussions. We also thank E. Ariel and A. Sharp for professional support in the flow cytometric analysis, T. Volberg for expert assistance with microscopy, and D. Resnitzky and O. Yarden for critical reading of the manuscript.

REFERENCES

1. **Almouzni, G., and A. P. Wolffe.** 1995. Constraints on transcriptional activator function contribute to transcriptional quiescence during early *Xenopus* embryogenesis. EMBO J. **14:**1752–1765.
2. **Bitzur, S., Z. Kam, and B. Geiger.** 1994. Structure and distribution of N-cadherin in developing zebrafish embryos: morphogenetic effects of ectopic over-expression. Dev. Dyn. **202:**121–136.
3. **Eaton, R., and R. D. Farley.** 1974. Spawning cycle and egg production of zebrafish, *Bracydanio rerio*, in the laboratory. Copeia **1:**195–209.
4. **Edgar, B. A., C. P. Kiehle, and G. Schubiger.** 1986. Cell cycle control by the nucleo-cytoplasmic ratio in early *Drosophila* development. Cell **44:**365–372.
5. **Edgar, B. A., and P. H. O'Farrell.** 1990. The three postblastoderm cell cycles of *Drosophila* embryogenesis are regulated in G2 by *string*. Cell **62:**469–480.
6. **Edgar, B. A., and G. Schubiger.** 1986. Parameters controlling transcriptional activation during early *Drosophila* development. Cell **44:**871–877.
7. **Foe, V. E., and B. M. Alberts.** 1983. Studies of nuclear and cytoplasmic behavior in the five mitotic cycles that precede gastrulation in *Drosophila* embryogenesis. J. Cell Sci. **61:**31–70.
8. **Fredrick, D. L., and M. T. Andrews.** 1994. Cell cycle remodeling requires cell-cell interactions in developing *Xenopus* embryos. J. Exp. Zool. **270:**410–416.
9. **Graham, C. F., and R. W. Morgan.** 1966. Changes in the cell cycle during early amphibian development. Dev. Biol. **14:**439–460.
10. **Graves, B. J., and G. Schubiger.** 1982. Cell cycle changes during growth and differentiation of imaginal leg discs in *Drosophila melanogaster*. Dev. Biol. **93:**104–110.
11. **Halevy, O., B. G. Novitch, D. B. Spicer, S. X. Skapek, J. Rhee, G. J. Hannon, D. Beach, and A. B. Lassar.** 1995. Correlation of terminal cell cycle arrest of skeletal muscle with induction of p21 by MyoD. Science **267:**1018–1021.
12. **Harper, J. W., and S. J. Elledge.** 1996. Cdk inhibitors in development and cancer. Curr. Opin. Genet. Dev. **6:**56–64.
13. **Kane, D. A., and C. B. Kimmel.** 1993. The zebrafish midblastula transition. Development **119:**447–456.
14. **Kane, D. A., R. M. Warga, and C. B. Kimmel.** 1992. Mitotic domains in the early embryo of the zebrafish. Nature (London) **360:**735–737.
15. **Kimmel, C. B., W. W. Ballard, S. R. Kimmel, B. Ullmann, and T. F. Schilling.** 1995. Stages of embryonic development of the zebrafish. Dev. Dyn. **203:**253–310.
16. **Kimmel, C. B., and R. D. Law.** 1985. Cell lineage of zebrafish blastomeres. I. Cleavage pattern and cytoplasmic bridges between cells. Dev. Biol. **108:**78–85.
17. **Kornberg, R. D., and Y. Lorch.** 1991. Irresistible force meets immovable object: transcription and the nucleosome. Cell **67:**833–836.
18. **Lukas, J., J. Bartkova, M. Rohde, M. Strauss, and J. Bartek.** 1995. Cyclin D1 is dispensable for G1 function in retinoblastoma gene-deficient cells independently of cdk4 activity. Mol. Cell. Biol. **15:**2600–2611.
19. **Marrable, A. W.** 1965. Cell numbers during cleavage of the zebra fish egg. J. Embryol. Exp. Morphol. **14:**15–24.
20. **McKnight, S. L., and O. L. Miller, Jr.** 1977. Electron microscopic analysis of chromatin replication in the cellular blastoderm *Drosophila melanogaster* embryo. Cell **12:**795–804.
21. **Newport, J., and M. Kirschner.** 1982. A major developmental transition in early *Xenopus* embryos: I. Characterization and timing of cellular changes at the midblastula stage. Cell **30:**675–686.
22. **Newport, J., and M. Kirschner.** 1982. A major developmental transition in early *Xenopus* embryos. II. Control of the onset of transcription. Cell **30:**687–696.

22a. **Pharan, N. B. Geiger, S. Zalik, Z. Kam, and A. Yarden.** Unpublished data.

23. **Prioleau, M. N., R. S. Buckle, and M. Mechali.** 1995. Programming of a repressed but committee chromatin structure during early development. EMBO J. **14:**5073–5084.
24. **Prioleau, M. N., J. Huet, A. Sentenac, and M. Mechali.** 1994. Competition between chromatin and transcription complex assembly regulates gene expression during early development. Cell **77:**439–449.
25. **Resnitzky, D., and S. I. Reed.** 1995. Different roles for cyclins D1 and E in regulation of the G_1-to-S transition. Mol. Cell. Biol. **15:**3463–3469.
26. **Rupp, R. A. W., and H. Weintraub.** 1991. Ubiquitous MyoD transcription at the midblastula transition precedes induction dependent MyoD expression in presumptive mesoderm of *X. laevis*. Cell **65:**927–937.
27. **Sánchez, I., and B. D. Dynlacht.** 1996. Transcriptional control of the cell cycle. Curr. Opin. Cell Biol. **8:**318–324.
28. **Sherr, C. J.** 1995. D-type cyclins. Trends Biochem. Sci. **20:**185–190.
29. **Sherr, C. J., and J. M. Roberts.** 1995. Inhibitors of mammalian G1 cyclin-dependent kinases. Genes Dev. **9:**1149–1163.
30. **Vasiliev, J. M., I. M. Gelfand, L. V. Domnina, and R. I. Rappoport.** 1969. Wound healing processes in cell cultures. Exp. Cell Res. **43:**83–93.
31. **Weinberg, R. A.** 1995. The retinoblastoma protein and cell cycle control. Cell **81:**323–330.
32. **Westerfield, M.** 1994. The zebrafish book, a guide for the laboratory use of zebrafish (*Brachydanio rerio*). University of Oregon Press, Eugene.
33. **Yarden, A., D. Salomon, and B. Geiger.** 1995. Zebrafish cyclin D1 is differentially expressed during early embryogenesis. Biochim. Biophys. Acta **1264:**257–260.